Received: 22 December 2021 | Revised: 28 November 2022 | Accepted: 15 March 2023

DOI: 10.1111/jfr3.12907

ORIGINAL ARTICLE

CIWEM Chartered Institution of Water and Environmental Management Journal of Flood Risk Management WILEY

Flood risk in Kuala Lumpur, Malaysia: A consideration of flood defences in a broadscale hydraulic model

Ashleigh Massam[1] | **Helen Smith**[1] | **Valeriya Filipova**[1] | **Simon Waller**[1] | **Nurfashareena Muhamad**[2] | **Joy Jacqueline Pereira**[2]

[1]JBA Risk Management, Skipton, UK

[2]Southeast Asia Disaster Prevention Research Initiative (SEADPRI), Institute for Environment & Development (LESTARI), Universiti Kebangsaan Malaysia, Kuala Lumpur, Malaysia

Correspondence
Ashleigh Massam, JBA Risk Management, Skipton, UK.
Email: ashleigh.massam@jbarisk.com

Funding information
Newton Ungku Omar Fund, Grant/Award Number: EP/P015506/1

Abstract

A novel approach to consider local-scale defence infrastructure in an urban environment, coupled with a broadscale hydraulic model framework, is applied to the capital city of Kuala Lumpur, Malaysia. Broadscale hydraulic modelling frameworks are often able to employ more complex models, but are typically limited to homogenous decision-making to ensure standardised outputs across large regions. Conversely, small-scale hydraulic modelling frameworks tend to better integrate local-scale features but can be computationally expensive to scale up beyond a regional view. Improvements to the broadscale hydraulic model framework through the incorporation of defence systems yield a more accurate representation of fluvial flood risk. This study incorporates defences in Kuala Lumpur, yielding a reduction in our estimates of fluvial flood extent by around 40%. The results of this study are validated against a set of high-quality observations, demonstrating the capability of the model framework in capturing flood risk in more than 95% of known flood risk zones in the city. Incorporating defence infrastructure using data-driven decision making and existing functionality in the hydraulic model could be automated in future model builds. This new approach bridges the gap between local-scale model frameworks and the broadscale, homogenous 2D hydraulic modelling studies.

KEYWORDS

disaster risk reduction, flood defence measures, fluvial, hydraulic modelling

1 | INTRODUCTION

Flood hazard maps are pivotal to flood risk management. In recent years, progress in the development of hydraulic model frameworks means we have the capacity to model flood risk on a global scale, using consistent approaches in an increasingly computationally efficient way (Dottori et al., 2016; Sampson et al., 2015). Here we present a data-driven approach within a broadscale model framework, using the existing functionality in a 2D full-Shallow Water Equation (full-SWE) hydraulic model to incorporate defences into a model configuration. This

framework is used to generate commercial flood maps with global coverage at a high resolution (5–30 m). We define broadscale as a framework that reuses a set of common assumptions to deliver multiple views of risk across a large region. Model parameterisation is generalised to be geographically inclusive. By contrast, a local study is customisable to specific geographic features, reducing the number of assumptions required in the model set-up. This study presents an approach to incorporating local-scale features into a broadscale model framework, which improves the accuracy of the estimated flood risk without compromising the simplicity of a broadscale configuration. The results of this study successfully demonstrate the potential of this model framework so that data-driven automated systems should, in the future, consider the incorporation of the high-quality defence data that is increasingly available in the big data era.

The combination of improved computational capacity, advances in model efficiency and the availability of big data makes the ambition of automating a high-resolution hydraulic model of the globe more realistic today than ever before (Alfieri et al., 2017; Dottori et al., 2016; Sampson et al., 2015; Wing et al., 2018). The computational expense of 2D full-SWE hydraulic models is reducing with the implementation of GPUs and parallelisation of code functionality (Crossley et al., 2010; Lamb et al., 2009; Neal et al., 2018). Two-dimensional (2D) hydraulic models yield accurate reconstructions of floodwater flow across a floodplain, and can appropriately consider obstructions in flow that are common in urban environments by modelling the flow of water in two dimensions (Fewtrell et al., 2008; Hocini et al., 2021; Hunter et al., 2008; Kirstetter et al., 2021). The reduction in expense is already making the application of 2D full-SWE hydraulic models a more popular choice for local-scale urban studies (Fewtrell et al., 2008; Henonin et al., 2013; Leandro et al., 2009).

Whilst the option for small-scale studies to apply 2D hydraulic models is getting easier, broadscale modelling studies that already employ 2D hydraulic models have the opportunity to improve how they consider local features. We define broadscale as a framework that reuses a set of common assumptions to deliver multiple views of risk across a large region. Model parameterisation is generalised to be geographically inclusive. Broadscale models can benefit from the availability of high-quality commercial and open-source "big data" whilst harnessing the power to automate. The combination of broadscale studies and automated model builds means the incorporation of local-scale features is now more accessible to global modelling frameworks (Towe et al., 2020; Trigg et al., 2016). This study demonstrates the potential of open-source repositories of flood defence data in a broadscale model framework by evaluating multiple views of flood risk that consider different types of defence infrastructure across a large region in Malaysia.

Flood defence systems are a key component to understanding flood risk, but are routinely removed or ignored to achieve homogeneity in a broadscale hydraulic model build. Instead, standalone defence datasets can be applied at a later point in the processing framework. The key reasons for the exclusion of defences are:

i. Few organisations collate information about defences; information is typically either held by several uncoordinated bodies, or not collated at all.
ii. The process of creating a high-quality global defence dataset is labour-intensive.
iii. The approach required to include defence systems in a hydraulic model will vary dependent on the type of defence and the model employed.
iv. Not all defence systems can be considered reliable in a real event, and end-users might prefer to use a "worst-case" flood scenario when quantifying risk or adopt a probabilistic approach using fragility curves.
v. Not all defence types can be explicitly modelled in a 2D hydraulic model.

All defence types are routinely represented in hydraulic models, often within linked 1D–2D models (Ferrari et al., 2020; Wing et al., 2019). Work is underway to be able to dynamically model defence systems in a 2D hydraulic model (Shustikova et al., 2020), however so far there is no single approach that can incorporate all defence types into a model. Defence datasets consist of an assortment of defence-type structures, such as levees, fixed and demountable defences, culverts and diversion canals and larger stormwater tunnels.

We present an approach to consider complex floodwater diversion systems in Kuala Lumpur, Malaysia, to estimate a more realistic view of the flood risk across the city. The Sendai Framework for Disaster Risk Reduction from 2015 to 2030 identifies climate change and rapid urbanisation as disaster risk drivers (UNISDR, 2015). Warming temperatures due to climate change will lead to an increase in rainfall event frequency and intensity in most areas, leading to more events that incur flood (IPCC, 2018). In Southeast Asia, monsoon precipitation is projected to increase in the mid-to long term (IPCC, 2021). Estimates of global economic and human loss from river flooding, even in the idealised climate change scenario of 1.5°C warming, could increase by 160%–240% (Dottori et al., 2018). In Kuala Lumpur, the urbanisation of the city over the last three decades corresponds with an intensification of short-duration heavy

rainfall events (Li et al., 2020). The intensification of rainfall is proving that the Kuala Lumpur region is already susceptible to the disaster risk drivers—across 2003–2015, 76 flash flood events were identified from government reports (Li et al., 2020; Wan Mohtar et al., 2020).

As a result of the increased flood risk to the city of Kuala Lumpur, the Malaysian government has made significant investments to flood defence infrastructure. The Stormwater Management and Road Tunnel (hereafter the SMART system) is a 9.7 km stormwater bypass tunnel with a 4 km dual-deck motorway within the tunnel (Abdullah, 2004a). The SMART system is the longest dual-purpose tunnel in the world, designed to solve the problem of both flash flooding and congestion in downtown Kuala Lumpur. The SMART system has different modes of activation. Depending on the activation mode, traffic will continue to use the tunnel whilst stormwater drains from the inflow point at the Berembang Pond (Klang River) to the outflow point at Desa Pond (Kerayong River). The activation mode is determined by the intensity of rainfall and river flow rates at the L4 gauge, upstream of the tunnel inlet.

This study presents flood hazard maps, developed as part of the study "Disaster Resilient Cities: Forecasting Local Level Climate Extremes and Physical Hazards for Kuala Lumpur"—an interdisciplinary 3-year project developed through a partnership of UK and Malaysian academic, industry and local government institutions, supported by UKRI, Innovate UK and the Malaysian Industry-Government Group for High Technology (MIGHT).

2 | METHODS

The JFlow hydraulic model is configured to produce four views of flood risk for fluvial (defended), fluvial (undefended) and direct rainfall events. The four views of risk represent events of increased magnitude with a recurrence probability of 1 in 20, 50, 100 and 200 years (the return period). The defended fluvial configuration considers flood protection systems including levees, diversion tunnels and canals and culverts.

2.1 | Location

This article presents a 5 m resolution flood map for fluvial and pluvial flood risk that covers the region administered by the City Hall of Kuala Lumpur (Dewan Bandaraya Kuala Lumpur, hereafter DBKL, Figure 1). The catchment dynamics of the DBKL region are influenced by the Klang River and its subsidiary the Gombak River, which meet at a confluence in downtown Kuala Lumpur. The city itself is located in the central part of the Klang Basin, which drains an area of 1288 km^2. Even though the upstream portion of the catchment is covered by tropical forest, more than 35% of the area is urbanised as a result of a rapid increase in population in the last 50 years.

The mean annual rainfall in the Klang Basin ranges from 2200 mm in the coastal area to 2700 mm in the mountains; this increase is most likely due to orographic enhancement. The mean annual temperature ranges from 22°C in the highlands to 26°C in the coastal area.

2.2 | Hydrology

2.2.1 | Fluvial hydrographs

Streamflow data for 10 gauges is available within the basin and the record lengths vary between 28 and 45 years. As an initial step, the non-parametric Mann Kendal and Pettit tests are applied to the extracted annual maxima (AMAX) series to check for monotonic trends and change points (abrupt changes in the mean; Pohlert, 2018). The results are significant for the majority of the gauges, likely due to rapid urbanisation within the region. Therefore, non-stationary analysis is applied for these gauges as the AMAX data does not comply with the assumption of the stationary flood frequency analysis of identically distributed values. The method involves fitting Generalised Additive Models for Location, Scale and Shape (GAMLSS) to estimate the parameters of a log-normal distribution (Stasinopoulos & Rigby, 2007). This approach is described in more detail in Filipova (2019). The distribution parameters are estimated from covariates using monotonic link functions. Based on results of other studies (Debele et al., 2017), the identity function was used for the mean and the log function for the standard deviation. Although it is possible to use a time series of land cover changes, no such dataset is available and therefore the only covariate is time. The log-normal distribution is used for all other sites where no trend is present. Even though the log Pearson type III distribution has been used in other studies in Malaysia (Hong Jer Lang et al., 2016), we chose the log-normal distribution to represent the limited available gauge data with a parsimonious model.

For gauged basins, the target flood peak quantiles (5, 20, 50, 100 and 200) are predicted through the application of fitted distributions under current conditions. The time to peak at each gauge is calculated by taking the median time to peak of all flood events, where the peak

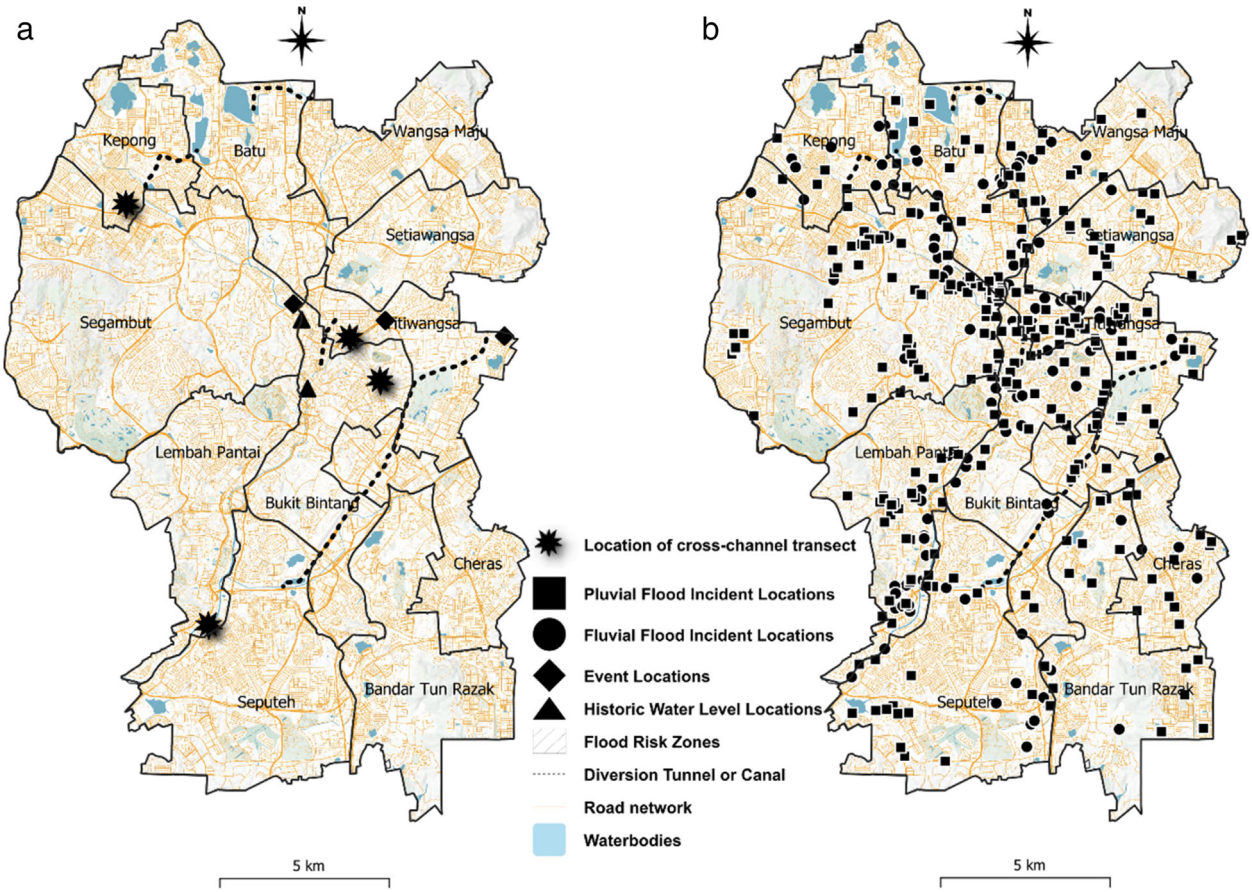

FIGURE 1 Left hand image: map of Kuala Lumpur marking the locations of historic water level, rainfall event and channel transect locations. A maximum flow rate is available for all diversion tunnels or canals (dashed lines). Right hand image: the same map of Kuala Lumpur with point locations of fluvial and surface water flood incidents spanning 1977–2020. Basemap created using ©Mapbox ©OpenStreetMap.

exceeds the 90th quantile of the flow series. The target flood peak quantiles at the ungauged sites are based on regression-based estimates, relating catchment area to the predicted flows at the gauged sites. Another regression equation is applied to all ungauged sites within the basin, relating the time to peak to the catchment area.

Flood hydrographs for selected return periods are calculated at 2-km intervals along the river channel. Each hydrograph is assumed to have a triangular profile, defined by time to peak and peak flow. A triangle hydrograph is a simple representation of discharge. This study calculates the maximum water depth in each cell of the model domain, throughout the duration of each simulation. The time of maximum inundation is not of concern when producing this type of hazard map. Further, a simple hydrograph is appropriate in a broadscale model framework for data-poor regions and to balance computational requirements with efficiency (Alfieri et al., 2014; Dottori et al., 2016; Sampson et al., 2015; Smith et al., 2015; Wing et al., 2017). This study reconstructs flood risk using a framework designed for the generation of commercial flood maps with global coverage. As a result, decisions on the shape of the hydrograph must consider data availability.

2.2.2 | Rainfall hyetographs

Rainfall hyetographs for the selected return periods are calculated on a 110 m × 110 m grid across the DBKL region. Following a process of evaluation and cleaning, data for 11 gauges are available within the 100 km^2 area centred on the middle of Kuala Lumpur. These gauges have hourly rainfall records that are at least 98% complete for a 20-year period, except for two stations that have only a 10-year record length. Each gauge record is analysed to extract the highest independent storm rainfall totals that exceed a certain threshold; this is done separately for 1-, 3- and 24-h storm durations at each gauge. A preference for a minimum of 300 records in each time series and the use of visual diagnostic tests guides the choice of minimum rainfall threshold used at each gauge

(Coles, 2001). The peaks over threshold are then fitted to a Generalised Pareto Distribution (GPD). The Grimshaw method is used to determine the maximum likelihood estimates for each of the GPD parameters as a function of extreme rainfall threshold (Grimshaw, 1993), thus enabling rainfall return levels to be deduced at each gauge for each of the three storm durations.

To calculate return levels at ungauged locations, ordinary kriging is used to spatially interpolate between the rainfall totals at each gauge, resulting in a continuous raster rainfall surface for each return period and storm duration at 110 m resolution. Use of inverse distance weighting (IDW) was also examined for spatial interpolation but produced a higher mean error and higher root mean square error. The gridded rainfall totals created by ordinary kriging are then converted into hyetographs describing the temporal distribution of rainfall for each of the three storm durations. A separate normalised rainfall profile is calculated for the 3- and 24-h storm durations by analysing hourly rainfall data for 20 events between 1997 and 2016 across the 11 rain gauge sites in Kuala Lumpur, plus an additional six gauges from the surrounding Selangor state. The graphical normalised profiles are the mean normalised profile across the 17 gauges. Due to the lack of sub-hourly rainfall data, the rainfall profile for the 1-h storm is assumed to be a simple triangular shape. As discussed in the fluvial hydrology section, this assumption is appropriate when using hyetographs as input to hydraulic models where the required output is maximum flood inundation (as opposed to time of maximum inundation).

2.3 | Hydraulic model

2.3.1 | Hydraulic model set-up

This study uses JFlow, a 2D full-SWE hydraulic model (Lamb et al., 2009). Separate fluvial and direct rainfall model configurations provide flood depths and extents based on specific flood type. The fluvial configuration is for all streams and rivers with the exception of very small streams, for which the flood extent and depths is derived from the direct rainfall configuration. Very small watercourses are defined as having a drainage area <3 km^2. The combination of flood extents and depths for small streams and fluvial outputs presents the flood risk for all rivers.

The City Hall of Kuala Lumpur provided a 0.5 m resolution bare-earth DEM of the DBKL region. To reconstruct a comprehensive view of the catchment dynamics, the fluvial hydraulic model reconstructs flood risk for the Klang Basin. To achieve this spatial coverage, 0.5 m Lidar data is supplemented with freely available SRTM data. The DEM is resampled to 5 m for modelling efficiency; this scale is commensurable with the size of individual buildings. The model configuration can simulate any number of views of severity. This study presents flood risk for 12 scenarios in total: four fluvial (defended), four fluvial (undefended) and four direct rainfall. Four scenarios represent return periods of increasing magnitude: 20, 50, 100 and 200. For each model configuration, broad-scale parameterisations are applied to all return periods and defended or undefended configurations (Table 1).

TABLE 1 Hydraulic model framework set-up.

	Fluvial		Small streams	Direct rainfall
Input	**Defended**	**Undefended**		
DEM	Bare Earth Lidar resampled to 5 m. 5 m SRTM outside of DBKL boundary.	Bare Earth Lidar resampled to 5 m (levees removed). 5 m SRTM outside of DBKL boundary.	Bare Earth Lidar resampled to 5 m (levees removed)	Bare Earth Lidar resampled to 5 m (levees removed)
Model Type	JFlow (2D full-SWE) fluvial configuration	JFlow (2D full-SWE) fluvial configuration	JFlow (2D full-SWE) direct rainfall configuration	JFlow (2D full-SWE) direct rainfall configuration
Defences	Levees SMART diversion tunnel Keroh diversion canal Batu diversion canal Bunus culvert Culverts <200 m in length Blockages	Culverts <200 m in length Blockages	Levees Culverts <200 m in length Blockages	Levees Culverts <200 m in length Blockages
Hydrology	3-step hydrograph	3-step hydrograph	Total rainfall estimates (spatial grid at 100 m resolution)	Total rainfall estimates (spatial grid at 100 m resolution)

The broadscale parameterisations ensure that hydraulic model configurations are uniform across model regions.

2.4 | Defences

The defended view of fluvial flood risk considers levee defences and SMART system. Levees are already present in the bare earth elevation model. As a result, an unprocessed bare earth DEM represents a somewhat-defended view of flood risk. For infrastructure, the impact of SMART defences is reconstructed by application of existing hydraulic model functionality to the defended model configuration.

2.4.1 | Defence systems considered in fluvial approach

The culvert functionality in JFlow software models the transportation of floodwater through the floodwater diversion systems in the DBKL region. Literature and data provided by consortium collaborators, enabled the identification of four major diversion tunnel or canals in the DBKL region (Abdullah, 2004a, 2004b; Varadharajan & Bailey, 2013). The model uses a culvert functionality that allows water to flow through the culvert, up to a theoretical maximum discharge. The actual discharge will depend on the availability of water. Water is only permitted to flow in one direction. A constant Manning's *N* coefficient of 0.04 represents concrete structures; channel length and flow rates are determined by records found in published literature (Table 2; Abdullah, 2004a; Varadharajan & Bailey, 2013). Accurate positioning of the tunnel and canals is achieved using satellite imagery.

Floodwater enters the SMART bypass tunnel by a holding pond at the inlet, the Berembang Pond and travels 9.7 km south to the outlet pond, the Desa Pond. Floodwater is released back into the river network via the Kerayong River. The SMART bypass tunnel has four activation modes (Table 3). The activation modes allow the bypass tunnel to be dual-purpose—cars can continue to travel through the tunnel on an upper deck whilst floodwater is transported below. More information on the activation modes can be found at http://smarttunnel.com.my/operational-modes/ (SMART Tunnel, 2021). Consideration of the activation modes means this study can moderate the application of the diversion tunnel, thereby more accurately representing the defence systems and their effect on flood risk in an urban environment.

TABLE 2 Defence system model parameterisations.

	SMART system	Keroh	Batu	Bunus
Channel type	Discharge limited directional	Discharge limited directional	Discharge limited directional	Rectangular
Manning's *N*	0.04	0.04	0.04	0.04
Flow rate ($m^3 s^{-1}$)	280.00	100.00	275.00	45.00
Length of channel geometry (m)	10,349.10	2246.00	4577.40	1520.10

TABLE 3 SMART bypass tunnel activation modes and equivalent return periods.

SMART mode	Weather condition	Flow at stream gauge at confluence of Klang and Ampang rivers ($m^3 s^{-1}$)	Flow of water expected to continue downstream of inlet pond ($m^3 s^{-1}$)	Associated return period
1	Fair	<70	N/A	RP20–RP200 (undefended)
2	Moderate rainfall	70–150	50	RP20 and RP50 (defended)
3	Major storm (tunnel reopens in 6–8 h)	>150	10	N/A
4	Prolonged heavy rain (tunnel reopens within 48 h)	>150	10	RP100, RP200, and RP1500 (defended)

2.4.2 | Levee identification and removal

One approach to homogenising models in a broadscale framework is to remove all organic defence structures (levees, embankments, dykes, all hereafter referred to as levees) that could be present in the DEM. Incorporation of levees in high resolution terrain data can be lost when resampling the DEM to the model resolution (typically 5–30 m for commercial global flood maps). Any inconsistency in the consideration of levees in a hydraulic model will have an impact on how one reliably interprets floodplain dynamics and connectivity (Scheel et al., 2019). To standardise the broadscale set-up whilst accounting for the variability in quality of available elevation data, levees are removed from the DEM using a variety of methods ranging from simple analytical algorithms (Passalacqua et al., 2012; Steinfeld et al., 2013; Wing et al., 2019) to more complex machine learning models (Wood et al., 2021).

A predictive model that uses the U-Net deep neural network for image segmentation (Wood et al., 2021) identified 201 raised defence features in the DEM. Software tools interpolate across the area of a raster that is covered by a raised feature, using a buffer of 1 pixel (5 m in map units). The output of this procedure is a processed DEM with levees "removed" that can be used in an undefended hydraulic model. The defended hydraulic model uses the 5 m DEM with levee features intact.

2.4.3 | DEM modifications for blockages observed in the DEM

Analyses of satellite imagery show the widespread nature of small culverts across the urban area. We choose to represent small culverts (<200 m in length) using DEM edits rather than specifically modelling the flow through a tunnel. Defended and undefended model frameworks accept DEM modifications. Furthermore, the accumulation of water at blocked culverts would create an unrealistic representation of flooding, even in the undefended view.

Software automation can detect and add edits to the DEM to remove features that might block waterflows, for example, bridges not removed from the bare earth elevation model. Blockages are identified by assessing locations where high-quality rail, road and drainage network data intersect the river network. DEM edits are drawn as geospatial line string geometries. An analytical algorithm identifies the start- and end-points of the line string geometries, taking into account the average elevation along the channel before the intersection. This ensures the edit crosses a blockage that is present in the DEM. The 2D hydraulic model rasterises the vector line string and interpolates a new elevation value for every pixel between the corresponding start- and end-point on the DEM.

2.5 | Validation

Flood maps of return periods cannot be directly compared with real flood events, as the latter cannot always be attributed with a single return period. Similarly, validation against other flood maps of static return periods should be avoided as this exercise is highly self-referential. Instead, comparisons against measured or known data assess model performance against benchmark expectations. Figure 1 presents the locations of data used to validate the flood maps (more information in Table 4). The data cover a number of different formats: sub-daily historic water levels spanning 2007–2018, point locations of flood incidents spanning 1977–2020 and throughput flow rates on diversion tunnels and at river locations. To ensure the quality of the benchmark data used to validate the flood map, validation data must be from a peer-reviewed source or provided directly from the Malaysian Department of Irrigation and Drainage (DID).

3 | RESULTS AND DISCUSSION

3.1 | Model validation

Successful validation of the flood maps is critical to understanding the impact of incorporating local-scale features in a broadscale model. Without benchmark flood maps to compare our maps against, we demonstrate the success of our hydraulic model framework using a range

TABLE 4 Table of validation data used throughout development and analysis.

Datapoint ID	Description	Type of data
1	Batu diversion canal	Maximum flow rate
2	Keroh diversion canal	Maximum flow rate
3	SMART diversion tunnel	Maximum flow rate
4	Sungai Bunus culvert	Maximum flow rate
5	Tun Perak Bridge	Historical water levels
6	Jln Sultan Ismail	Historical water levels
8	JPS Ampang	Event history
9	PWTC	Event history
10	Jln Tun Razak	Event history
11	Flood incident points	Point locations of individual flood incidents

TABLE 5 Event dates, locations, total rainfall at specific locations in Kuala Lumpur.

Event date	Location (ID, description)	Water level location (ID, description)	Event duration (h)	Total rainfall (mm)	Effective return period	Nearest modelled return period
07/03/2012	8, JPS Ampang	5, Tun Perak	1	164	200	200
21/08/2012	9, PWTC	6, Jln Sultan Ismail	3	129	15	20
10/04/2013	10, Jln Tun Razak	5, Tun Perak	1	115	110	100
03/11/2013	9, PWTC	6, Jln Sultan Ismail	3	114.5	5	20

Note: Data provided by Wan Mohtar (pers. comms.), originally obtained from DID and used in Wan Mohtar et al. (2020). Effective return periods and event duration are estimated by linear interpolation between all rainfall grid rasters at the event location.

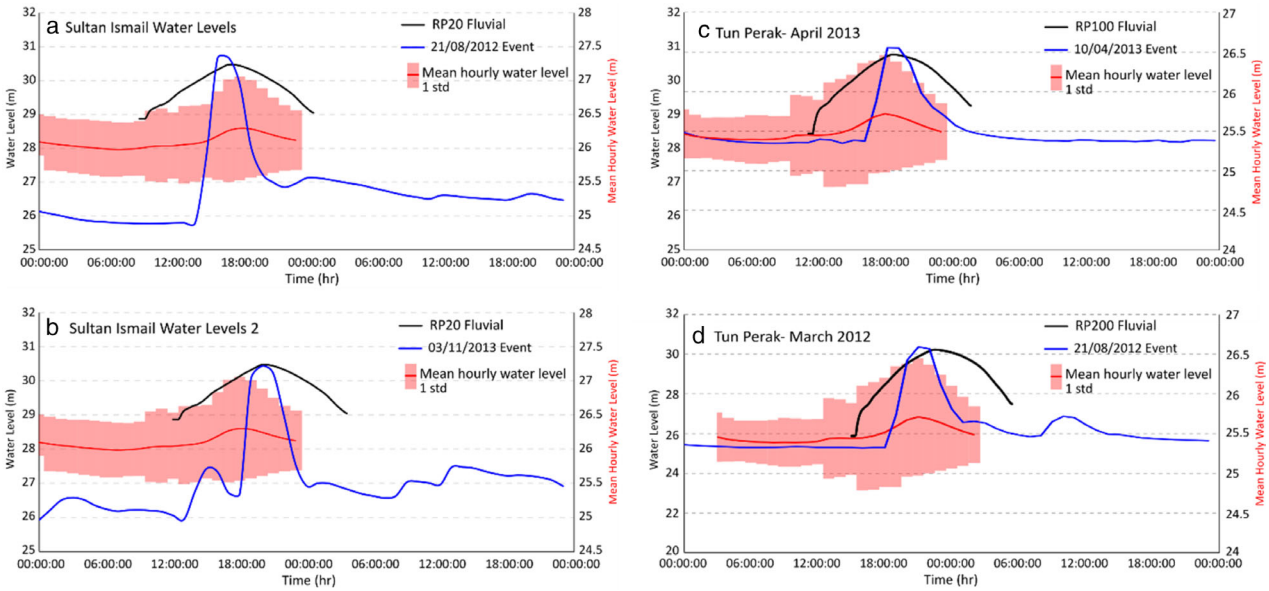

FIGURE 2 (a–d) Comparison plots of water level data for four flash flood events in the DBKL region. Blue: historic hourly data isolating the impact of the rainfall event in the water level record; Red (and pink shading): Mean hourly water level record and standard deviation for the water level time series; Black: modelled water level for the corresponding nearest modelled return period.

of data points and historic data at specific locations across the DBKL region.

3.1.1 | Comparison with historical flood events

Validation of the flood maps by comparison with historical flood events is an important step in proving the efficacy of the model reconstructions. The first assessment uses two independent datasets of flood information across Kuala Lumpur: an event repository, created as part of the study published by Wan Mohtar et al. (2020) and water level gauge records provided by the DID. The event repository provides the date, location, duration and total rainfall for several events within the historical time series (Wan Mohtar, pers corr.; Table 5). An effective return period for each event can be estimated by relating the recorded rate of rainfall to the rainfall hyetograph grids. Water level records at gauges across the DBKL region allow us to isolate historical events in water level records. The hydraulic model estimates of water depth for the nearest return period can be validated through comparison with the historical water level time series across an historical event. Comparison of four isolated events across the DBKL region with modelled water levels suggests a high degree of accuracy in the model's capability to estimate flood depths in these locations (Figure 2).

A second validation assessment uses a compilation of flood incidents spanning 1977–2020. The flood incident dataset has been split by fluvial and pluvial flood type (Figure 1). Analysing the flood maps using this dataset provides a broad spatial assessment of the flood maps at a high resolution. By applying a buffer of 20 m to each

point, nearly 92% of 569 locations are inundated by flood in the flood hazard maps. In total, 262, 276 and 418 incidents are within 20 m of flood for the defended fluvial, undefended fluvial and surface water hazard maps, respectively, with 125 incidents at risk of both fluvial and surface water flooding.

Assessment of the flood hazard maps against historical event data provides confidence that the model outputs identify flood risk across the DBKL region. Assessment against historic events does not yield information on the performance of defence systems as the event occurrence ranges pre- and post-construction of the SMART system. Separate validation on how defence infrastructure is represented in the model build evaluates the novel application of existing functionality to represent a variety of defence types.

3.1.2 | Discharge rates through culverts

We assess the defended model build by comparing flow hydrograph reconstructions at five locations. Flow is recorded through the culvert functionality at 0.1 h intervals during the model simulation. An additional extreme return period, RP1500, provides a more severe event in order to reconstruct the most extreme estimated flow rates at the L4 gauge, upstream of the inlet pond of the SMART bypass tunnel. The maximum capacity for diversion systems, as provided by the DID or in Abdullah (2004b), is included in each subplot for comparison. The model configurations do not constrain the length of simulated event time, instead allowing the model to run until it reaches a maximum depth in every domain cell (equivalent to the model resolution). As a result of this set-up in the hydraulic modelling framework, we assume activation mode 4 for every return period with a flow rate >150 $m^3 s^{-1}$ at the L4 gauge (see Table 3).

Reconstructions of maximum flow rates through the culverts suggest appropriate water retention and transport in the defended hydraulic model build (Figure 3). Of particular interest, the flood hazard maps demonstrate that negligible water flows downstream of the SMART inlet pond, suggesting that the DEM is able to affect appropriate water retention at the Berembang Pond. The successful floodwater capture at the Berembang Pond means all floodwater travels through the culvert that reconstructs the impact of the SMART bypass tunnel for release into the Desa Pond. Maintaining flow rates below the maximum threshold of 280 $m^3 s^{-1}$ at the outlet pond (Figure 3a; Abdullah, 2004b) minimises the risk of overspill at the Klang-Kerayong confluence. Flow rate measurements obtained during hydraulic model simulations at a location on the Kerayong River, downstream of the outlet pond, are consistently below the maximum acceptable threshold of 200 $m^3 s^{-1}$ (Abdullah, 2004b; Figure 3b). Assessment of the reconstructed flow hydrographs through the SMART system and at the outlet pond suggests that the model framework does not introduce artificial flood risk at the Klang–Kerayong confluence.

In satellite imagery, the Sungai Bunus appears to be a partially culverted tributary of the Klang River. We chose to reconstruct the Sungai Bunus using the most simplistic culvert functionality available in JFlow by making no assumptions on the flow of water, with the caveat that robust evidence of the culvert characteristics is lacking. Based on data provided by the DID, the maximum flow rate through the Sungai Bunus should not exceed 45 $m^3 s^{-1}$ (Abdullah, 2004b). Flow rates through the Sungai Bunus culvert nears but does not exceed the maximum capacity as cited in literature (Figure 3c).

In the case of flow rates through the Batu and Keroh diversion canals, the modelled rates are significantly lower than maximum capacity (Figure 3d,e). The low flow rates are likely attributable to model underperformance, due to the location of the diversion canals in the context of the model framework. The Keroh and Batu diversion canals are close to the northern boundary of the DBKL region (Figure 1). The upstream catchment dynamics for this location are modelled on lower quality SRTM elevation data. The quality of this elevation leads to 'pooling' in the hydraulic model that is not realistic and inevitably reduces the amount of water that flows downstream.

Comparison of the modelled flow hydrographs against known maximum flow rates allow for the validation of the application of culverts in the model set-up insofar as the model framework does not overestimate the capacity of each diversion system. Comparison of modelled data with known discharge rates through the tunnels and expected rates of flow downstream of inlet and outlet ponds confirm that the model set-up successfully reconstructs the water retention and diversion in Kuala Lumpur (Figure 3).

3.2 | Assessment of defended and undefended scenarios

This study seeks to prove that the application of defence infrastructure in automated, broadscale modelling frameworks provides a more accurate view of flood risk in the urban environment. The key differences between undefended and defended fluvial modelling framework are culvert activation and the DEM. As the focus of Kuala Lumpur flood resilience schemes is constrained to the

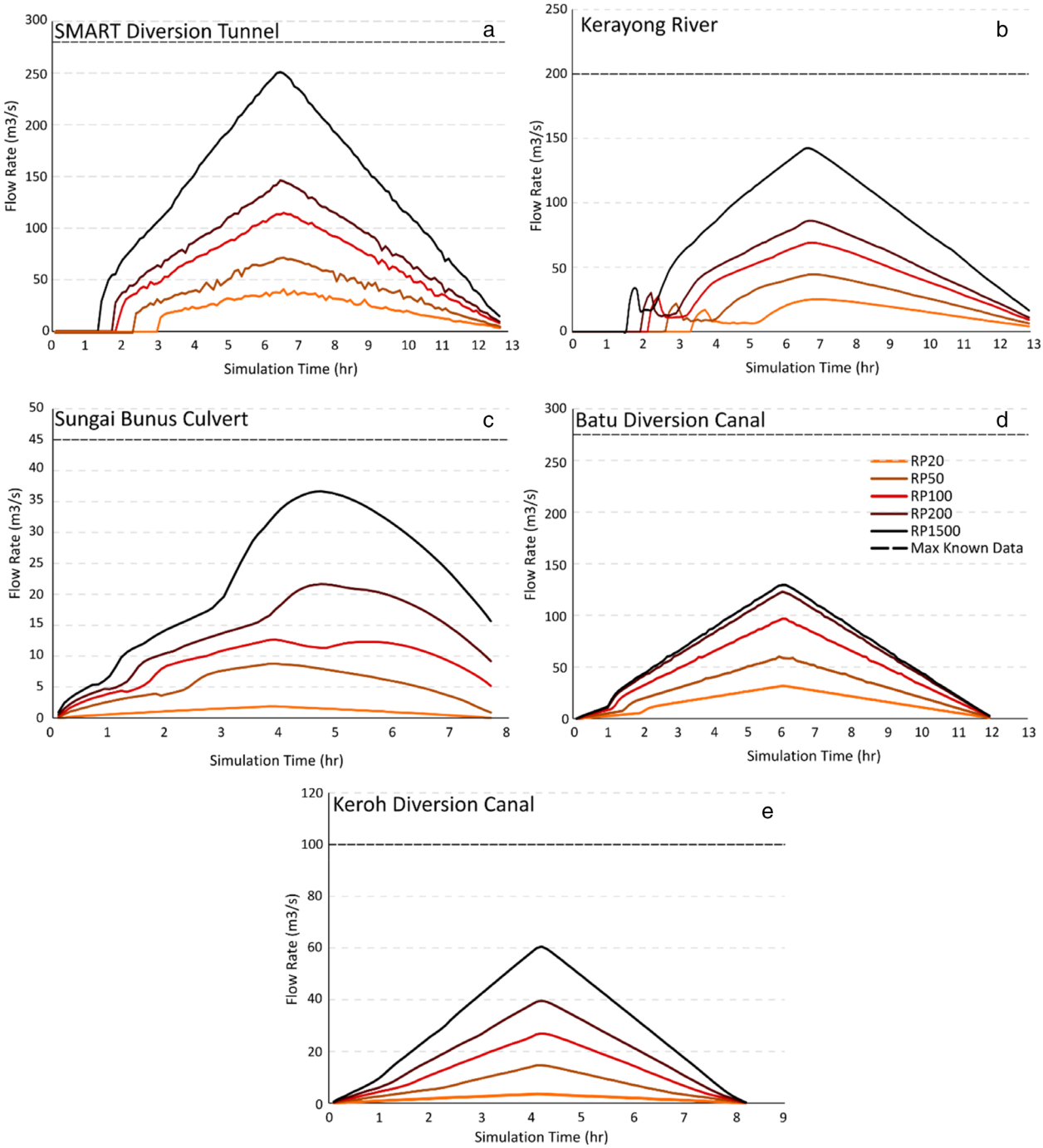

FIGURE 3 (a–e) Reconstructed flow hydrograph for duration of simulation for four culverts used to simulate diversion tunnels or canals in the DBKL region. Top row: (a) SMART diversion tunnel; (b) monitoring line data for a location on the Kerayong River downstream of the Desa Pond; (c) Sungai Bunus culvert; (d) Batu diversion canal; and (e) Keroh diversion canal. All sub-plots show reconstructed flow for all modelled return periods and the static maximum flow rate.

Klang River, the fluvial flood maps are consistent to a high degree. A Jaccard similarity coefficient of 0.88 indicates high correlation between flood extents in the RP200 scenarios across the DBKL region.

The defended model framework yields a reduction in flood extent of 15–24 km^2 (Table 6). The area west of the Berembang Pond benefits from the reduced flood extent and property damage in the defended model framework. This area (Figure 4a) is downstream of the inlet for the SMART tunnel, where the flow of water directed toward the Tun Perak bridge is reduced as a result of SMART activation. Assessment of the potential impact of a RP200

TABLE 6 Flood extent (in km^2) and the number of building affected by each flood type for RP20–RP200.

	RP20	RP50	RP100	RP200
All rivers (undefended)				
Area (km^2)	38.96	46.87	54.49	58.83
Buildings affected	12,468	14,733	16,299	17,437
All rivers (defended)				
Area (km^2)	23.94	28.52	32.34	35.20
Buildings affected	10,854	12,876	14,113	15,356
Small streams				
Area (km^2)	19.90	21.70	22.90	24.18
Buildings Affected	10,586	11,621	12,127	12,820
Surface water				
Area (km^2)	21.57	53.25	54.41	55.27
Buildings affected	41,781	41,748	41,856	41,712

flood on this areas suggests the defended view protects 1600–2200 buildings. Figure 5 supports the finding that flood defences in a broadscale hydraulic model framework can yield more realistic expectations on flood depth and flood extent. Four transects across the DBKL region show the impact of flood defences: Transects A and B show the consistent reduction in flood depth downstream of the SMART Tunnel and the Sungai Bunus culvert (Figure 5a,b). Transect C, at a location protected by levee defences near the Keroh diversion canal, demonstrates the impact that levee defences have on reducing flood extent. Water remains within the channel peaking at the same depth as the undefended scenario. However, water depths extend along the transect as water spills into an undefended flood plain in the undefended scenario.

There is evidence that additional flooding can occur downstream of the SMART outlet in the defended scenario. Figure 4b shows greater flood extents in the

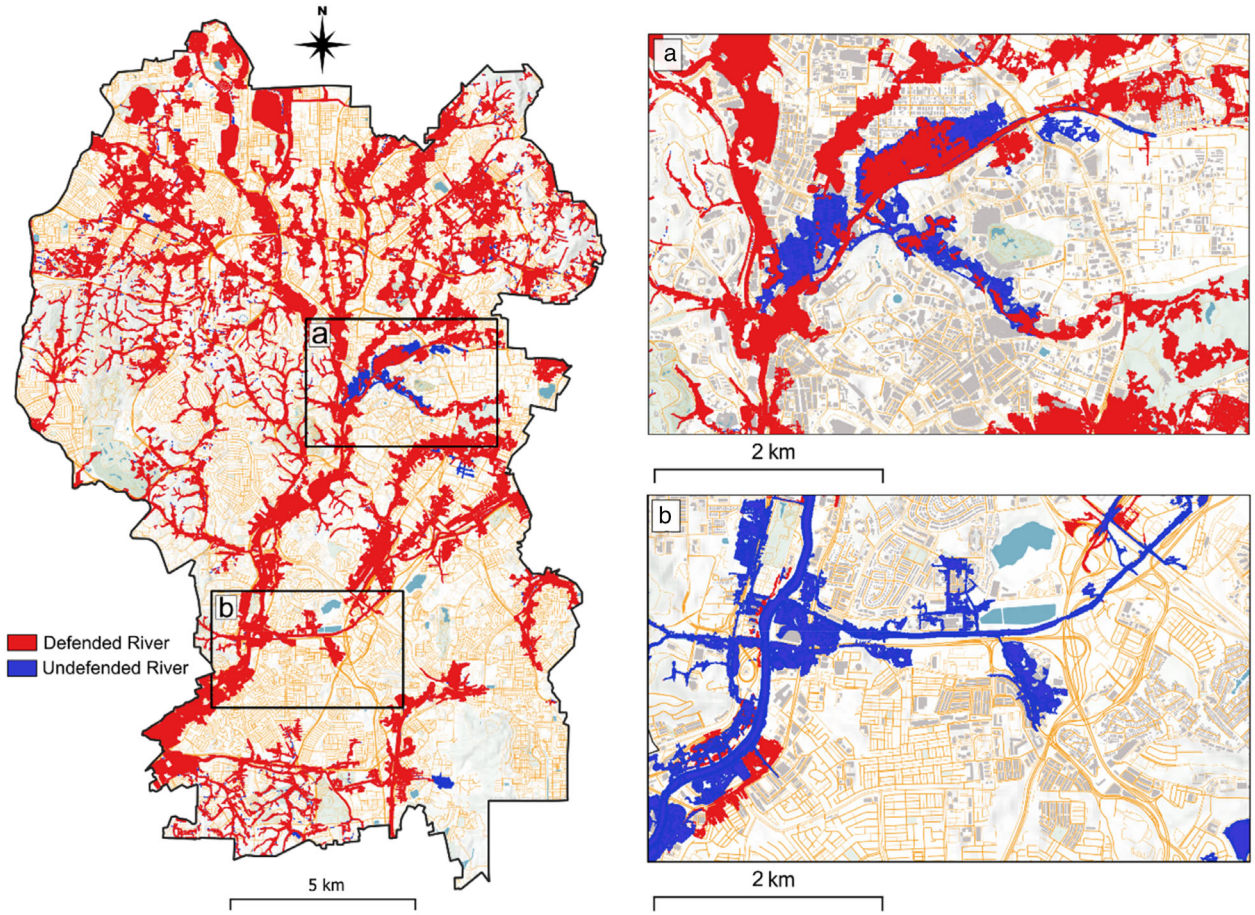

FIGURE 4 Clockwise from top-left: Flood extents across the DBKL region. Red: RP200 defended river extents; Blue: RP200 undefended river extents. Two boxes show the location of zoomed-in views of flood risk. Right Hand Image (a): A zoomed-in view of flood extents along the Klang River, downstream of the SMART inlet pond; (b) A zoomed-in view of flood extents along the Kerayong River, downstream of the SMART outlet pond. Basemap created using ©Mapbox ©OpenStreetMap.

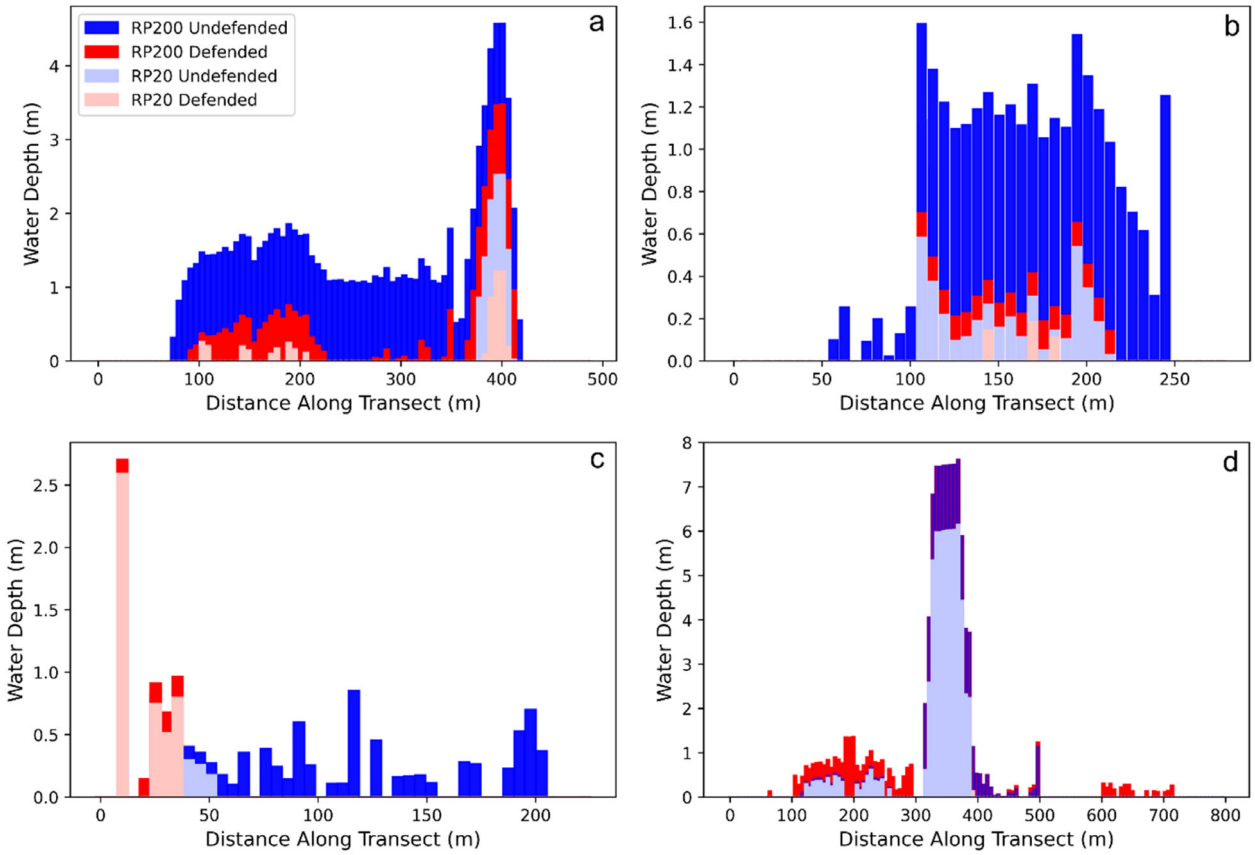

FIGURE 5 Flood depths for two return periods (RP20, RP200) for both the defended and undefended fluvial scenarios, taken along four transects from across the DBKL region. Clockwise from top-left: (a) downstream of the SMART inlet pond; (b) downstream from a culverted section of Sungai Bunus; (c) small stream defended by levees near the Keroh diversion canal; (d) downstream of the Klang-Kerayong confluence where levees were identified. Locations of each transect are labelled in Figure 1a. In plots (c) and (d), peaks in water depths at distances along the transects between 0–50 m and 300–400 m, respectively, appear as one scenario but depths are identical in both defended and undefended scenarios.

defended scenario in the most severe return period (RP200). Transect D (Figure 5d) supports this finding and suggests that the region is at risk of greater flood depths as well as extents. The increase in flood risk is likely the result of floodwater transported during SMART activation. As discussed in Section 3.1.2, the hydraulic model output maintains flow rates below a threshold to minimise the risk of overspill at the Klang–Kerayong confluence (Abdullah, 2004b). Literature published in the SMART planning phase suggests the Klang-Kerayong region would benefit from increased channel capacity and levee defences (Abdullah, 2004a); however, there is a data scarcity when it comes to confidently incorporating defence infrastructure into the model framework at this location. As a result, our findings suggest that this region is at greater flood risk as a result of the SMART defence systems. In the future, this flood risk could be reduced by defence systems that are not currently incorporated into the hydraulic model framework. The impact of this finding reinforces the importance of the availability of accurate and reliable information on defences.

Overall, the reduction in flood depths is a key impact of the SMART system. Across the DBKL region, our flood map estimates a mean water depth of 1.0–1.4 m in the undefended scenario, with a median depth of 0.4–0.7 m, across all return periods. In the defended fluvial scenario, the mean depths reduce to 0.8–1.0 m. However, SMART activation is able to maintain the median water depth at ~0.4 m across all return periods, suggesting that the key effectiveness of the SMART system activation modes is to control the transport and flow rate of floodwater across the city during severe events. This is evidenced in Figure 4a,b, where constraints on the range of flood depths across return periods reduces maximum flood depths in the defended scenarios to the equivalent of RP20 in the undefended view of flood risk. The scalability

of the SMART defence system to re-route variable volumes of floodwater whilst maintaining a median depth of ~0.4 m has a significant impact on the reduction of the cost of flood damage. Reducing flood depths ultimately reduces the amount of damage on a property as a result of flood. D'Ayala et al. (2020) estimate the cost of flood damage from a RP100 event on heritage buildings located in the Kampung Baru neighbourhood, located between the Klang and Bunus rivers, is reduced by RM 5 M (~€1 M). Despite limited variation in the flood extent, the variability across flood depths for the undefended scenario of 0.5–1.4 m is reduced to mostly 0.5–0.7 m (with a maximum depth of 1.1 m) in the defended scenario (D'Ayala et al., 2020).

In the case study of Kuala Lumpur, incorporation of defence infrastructure in the model framework reduces the fluvial flood extent across the whole region by 40%, with further reduction of flood depths in inundated areas. Both factors influence the estimated cost of damage incurred by flood. The positive impact of reliable defence infrastructure on flood risk should be readily incorporated into broadscale model frameworks so that users of the data can make more accurate estimates on the cost of flood damage.

3.3 | Opportunity for broadscale model frameworks

Continuous improvements to software architecture will enable data-driven decision making in a broadscale model build (Towe et al., 2020). Improved software architecture will enable us to integrate heterogeneous data stored in a common database. This would allow the incorporation of complex defence systems, by developing the means of a data-driven hydraulic model build. In simpler terms: local-scale defence systems could be included in a broadscale model, using software automation to select defence features from a common database and implement whatever model functionality is required. This advance in software development draws together the benefits of both local-scale and broadscale model builds (Towe et al., 2020).

This study develops an approach that marries the incorporation of local-scale features with the benefits of a broadscale 2D hydraulic model, with the intention of demonstrating the potential to include high-quality defence data into a global modelling framework. This new broadscale model framework should be adopted in future set-ups using a data-driven automated system, incorporating the high-quality defence data that is increasingly available in the "big data" era.

4 | CONCLUSIONS

This article presents the development of 5 m flood maps for Kuala Lumpur, Malaysia. The hydraulic model framework covered two types of flood: direct rainfall and fluvial flooding. For this study, two scenarios of fluvial flood risk were developed: the simplified broadscale 'undefended' view and a 'defended' view that accounts for the infrastructure investments already made by the city of Kuala Lumpur to mitigate flood risk. Flood maps were created using a 2D full-SWE hydraulic model under broadscale model assumptions, calibrated to local defence features.

Accurate representation of flood risk depends on the successful incorporation of model choice, elevation data and high-quality representation of local-scale features. Computationally-intensive models, such as the 2D full-SWE hydraulic model used in this study, provide more accurate representations of the flow and transportation of floodwater across floodplains. However, for successful continent-wide model frameworks, data and assumptions on local-scale features tend to be homogenous to improve efficiency in model set-up and simulation.

The defended fluvial flood map reduces the flood extent in Kuala Lumpur by 40% across all return periods, indicating overestimation of damage in an undefended scenario. Further, this study has demonstrated that existing model functionality is capable of reconstructing the impact of complex flood defence systems. Future broadscale model frameworks should aim to incorporate local-scale features using this approach, and advance on this work by adopting a data-driven decision-making schema that is capable of automating the application of heterogenous data formats.

ACKNOWLEDGEMENTS

The authors would like to thank Wan Hanna Melini Wan Mohtar at Universiti Kebangsaan Malaysia for providing flash flood event information for validation of the reconstructed water levels. The authors would like to thank Mark Saunders (UCL Department of Space and Climate Physics, Faculty of Maths and Physical Sciences) for providing normalised rainfall profiles and gridded rainfall return levels for the Kuala Lumpur study area, used by JBA to determine the hyetographs for the flood hazard simulations. This research has been supported with funding from the Newton Ungku Omar Fund administrated by Innovate UK and the Malaysian Industry-Government Group for High Technology (MIGHT) for the EPSRC project entitled "Disaster Resilient Cities: Forecasting Local Level Climate Extremes and Physical Hazards for Kuala Lumpur"

(EP/P015506/1). The authors would like to thank the anonymous reviewers, Associate Editor and Editor of the journal for their constructive input to this manuscript. We would also like to thank Professor Rob Lamb for his guidance during the process.

DATA AVAILABILITY STATEMENT

The data that support the findings of this study are available from the corresponding author upon reasonable request.

ORCID

Ashleigh Massam https://orcid.org/0000-0001-6138-4579

REFERENCES

Abdullah, K. (2004a). *Kuala Lumpur: Re-engineering a flooded confluence*. Fourteenth Professor Chin Fung Kee Memorial Lecture.

Abdullah, K. (2004b). Stormwater management and road tunnel (SMART) a lateral approach to flood mitigation works. In International conference on bridge engineering and hydraulic structures, Selangor, Malaysia.

Alfieri, L., Bisselink, B., Dottori, F., Naumann, G., de Roo, A., Salamon, P., Wyser, K., & Feyen, L. (2017). Global projections of river flood risk in a warmer world. *Earth's Futures*, *5*, 171–182. https://doi.org/10.1002/2016EF000485

Alfieri, L., Salamon, P., Bianchi, A., Neal, J., Bates, P., & Feyen, L. (2014). Advances in pan-European flood hazard mapping. *Hydrological Processes*, *28*(13), 4067–4077. https://doi.org/10.1002/hyp.9947

Coles, S. (2001). *An introduction to statistical modelling of extreme values* (p. 209). Springer-Verlag. https://doi.org/10.1007/978-1-4471-3675-0

Crossley, A., Lamb, R., & Waller, S. (2010). Fast solution of the shallow water equations using GPU technology. In S. Coles (Ed.), *An introduction to statistical modelling of extreme values*. British Hydrological Society.

D'Ayala, D., Wang, K., Yan, Y., Smith, H., Massam, A., Filipova, V., & Pereira, J. J. (2020). Flood vulnerability and risk assessment of urban traditional buildings in a heritage district of Kuala Lumpur, Malaysia. *Natural Hazards and Earth System Sciences*, *20*, 2221–2241.

Debele, S. E., Strupczewski, W., & Bogdanowicz, E. (2017). A comparison of three approaches to non-stationary flood frequency analysis. *Acta Geophysica*, *65*(4), 863–883. https://doi.org/10.1007/s11600-017-0071-4

Dottori, F., Salamon, P., Bianchi, A., Alfieri, L., Hirpa, F. A., & Feyen, L. (2016). Development and evaluation of a framework for global flood hazard mapping. *Advances in Water Resources*, *94*, 87–102.

Dottori, F., Szewczyk, W., Ciscar, J.-C., Zhao, F., Alfieri, L., Hirabayashi, Y., Bianchi, A., Mongelli, I., Frieler, K., Betts, R. A., & Feyen, L. (2018). Increased human and economic losses from river flooding with anthropogenic warming. *Nature Climate Change*, *8*, 781–786. https://doi.org/10.1038/s41558-018-0257-z

Ferrari, A., Dazzi, S., Vacondio, R., & Mignosa, P. (2020). Enhancing the resilience to flooding by levee breaches in lowland areas: A methodology based on numerical modelling. *Natural Hazards and Earth System Sciences*, *20*, 59–72. https://doi.org/10.5194/nhess-20-59-2020

Fewtrell, T. J., Bates, P. D., Horritt, M., & Hunter, N. M. (2008). Evaluating the effect of scale in flood inundation modelling in urban environments. *Hydrological Processes*, *22*(26), 5107–5118. https://doi.org/10.1002/hyp.7148

Filipova, V. (2019). *Non-stationary flood frequency analysis in Langat basin, Malaysia*. European Water Resources Association (EWRA).

Grimshaw, S. D. (1993). Computing maximum likelihood estimates for the generalised Pareto distribution. *Technometrics*, *35*, 185–191. https://doi.org/10.2307/1269663

Henonin, J., Russo, B., Mark, O., & Gourbesville, P. (2013). Real-time urban flood forecasting and modelling: A state of the art. *Journal of Hydroinformatics*, *15*(3), 717–735. https://doi.org/10.2166/hydro.2013.132

Hocini, N., Payrastre, O., Bourgin, F., Gaume, E., Davy, P., Lague, D., Poinsignon, L., & Pons, F. (2021). Performance of automated flood inundation mapping methods in a context of flash floods: A comparison of three methods based either on the height above nearest drainage (HAND) concept, or on 1D/2D shallow water equations. *Hydrological Earth Systems Science Discussions*, *25*(6), 2979–2995. https://doi.org/10.5194/hess-2020-597

Hong Jer Lang, D., Hanim bt Mohd Puad, A., Shafiliah bt Abdul Azia, I., & Kee An, H. (2016). Estimating generalised flood sew coefficients for peninsular Malaysia. *Journal – The Institution of Engineers*, *77*, 15–21.

Hunter, N. M., Bates, P. D., Neelz, S., Pender, G., Villanueva, I., Wright, N. G., Liang, D., Falconer, R. A., Lin, B., Waller, S., Crossley, A. J., & Mason, D. C. (2008). Benchmarking 2D hydraulic models for urban flooding. *Proceedings of the Institution of Civil Engineers: Water Management*, *161*(1), 13–30. https://doi.org/10.1680/wama.2008.161.1.13

IPCC. (2018). Impacts of 1.5°C global warming on natural and human systems. In V. Masson-Delmotte, P. Zhai, H. O. Pörtner, D. Roberts, J. Skea, P. R. Shukla, A. Pirani, W. Moufouma-Okia, C. Péan, R. Pidcock, S. Connors, J. B. R. Matthews, Y. Chen, X. Zhou, M. I. Gomis, E. Lonnoy, T. Maycock, M. Tignor, & T. Waterfield (Eds.), *Global warming of 1.5°C. IPCC special report on the impacts of global warming of 1.5°C above pre-industrial levels and related global greenhouse gas emission pathways, in the context of strengthening the global response to the threat of climate change, sustainable development, and efforts to eradicate poverty*. World Meteorological Organization.

IPCC. (2021). Summary for policymakers. In V. Masson-Delmotte, P. Zhai, A. Pirani, S. L. Connors, C. Péan, S. Berger, N. Caud, Y. Chen, L. Goldfarb, M. I. Gomis, M. Huang, K. Leitzell, E. Lonnoy, J. B. R. Matthews, T. K. Maycock, T. Waterfield, O. Yelekçi, R. Yu, & B. Zhou (Eds.), *Climate change 2021: The physical science basis. Contribution of working group I to the sixth assessment report of the intergovernmental panel on climate change*. Cambridge University Press.

Kirstetter, G., Delestre, O., Lagree, P.-Y., Popinet, S., & Josserand, C. (2021). B-flood 1.0: An open-source Saint-Venant model for flash flood simulation using adaptive refinement.

Geoscientific Model Development, 14(11), 7117–7132. https://doi.org/10.5194/gmd-2021-15

Lamb, R., Crossley, M., & Waller, S. (2009). A fast two-dimensional floodplain inundation model. *Proceedings of the Institution of Civil Engineers: Water Management*, *162*(6), 363–370.

Leandro, J., Chen, A. S., Djordjevic, S., & Savic, D. (2009). Comparison of 1D/1D and 1D/2D coupled (sewer/surface) hydraulic models for urban flood simulation. *Journal of Hydraulic Engineering*, *135*(6), 495–504. https://doi.org/10.1061/(ASCE)HY.1943-7900.0000037

Li, Y., Fowler, H. J., Argueso, D., Blenkinsop, S., Evans, J. P., Lenderink, G., Yan, X., Guerreiro, S. B., Lewis, E., & Li, X.-F. (2020). Strong intensification of hourly rainfall extremes by urbanisation. *Geophysical Research Letters*, *47*(14), 1–8. https://doi.org/10.1029/2020GL088758

Neal, J., Dunne, T., Sampson, C., Smith, A., & Bates, P. (2018). Optimisation of the two-dimensional hydraulic model LISFOOD-FP for CPU architecture. *Environmental Modelling & Software*, *107*, 148–157. https://doi.org/10.1016/j.envsoft.2018.05.011

Passalacqua, P., Belmont, P., & Foufoula-Georgiou, E. (2012). Automatic geomorphic feature extraction from lidar in flat and engineered landscapes. *Water Resources Research*, *48*, 1–18. https://doi.org/10.1029/2011WR010958

Pohlert, T. (2018). trend: Non-parametric trend tests and change-point detection. https://CRAN.R-project.org/package=trend

Sampson, C. C., Smith, A. M., Bates, P. D., Neal, J. C., Alfieri, L., & Freer, J. E. (2015). A high-resolution global flood hazard model. *Water Resources Research*, *51*(9), 7358–7381. https://doi.org/10.1002/2015WR016954

Scheel, K., Morrison, R. R., Annis, A., & Nardi, F. (2019). Understanding the large-scale influence of levees on floodplain connectivity using a hydrogeomorphic approach. *Journal of the American Water Resources Association*, *55*(2), 413–429.

Shustikova, I., Neal, J. C., Domeneghetti, A., Bates, P. D., Vorogushyn, S., & Castellarin, A. (2020). Levee breaching: A new extension to the LISFLOOD-FP model. *Water*, *12*(4), 942–959. https://doi.org/10.3390/w12040942

SMART Tunnel. (2021). *Operational modes*. http://smarttunnel.com.my/operational-modes/

Smith, A., Sampson, C., & Bates, P. (2015). Regional flood frequency analysis at the global scale. *Water Resources Research*, *51*(1), 539–553. https://doi.org/10.1002/2014WR015814

Stasinopoulos, D. M., & Rigby, R. A. (2007). Generalized additive models for location scale and shape (GAMLSS). *Journal of Statistical Software*, *23*(7). https://doi.org/10.18637/jss.v023.i07

Steinfeld, C. M. M., Kingsford, R. T., & Laffan, S. W. (2013). Semi-automated GIS techniques for detecting floodplain earthworks. *Hydrological Processes*, *27*, 579–591. https://doi.org/10.1002/hyp.9244

Towe, R., Dean, G., Edwards, L., Nundloll, V., Blair, G., Lamb, R., Hankin, B., & Manson, S. (2020). Rethinking data-driven decision support in flood risk management for a big data age. *Journal of Flood Risk Management*, *13*(4), 1–19. https://doi.org/10.1111/jfr3.12652

Trigg, M. A., Birch, C. E., Neal, J. C., Bates, P. D., Smith, A., Sampson, C. C., Yamazaki, D., Hirabayashi, Y., Pappenberger, F., Dutra, E., Ward, P. J., Winsemius, H. C., Salamon, P., Dottori, F., Rudari, R., Kappes, M. S., Simpson, A. L., Hadzilacos, G., & Fewtrell, T. J. (2016). The credibility challenge for global fluvial flood risk analysis. *Environmental Research Letters*, *11*, 1–11. https://doi.org/10.1088/1748-9326/11/9/094014

UNISDR. (2015). *Sendai framework for disaster risk reduction 2015–2030*. UNISDR.

Varadharajan, R. B., & Bailey, C. J. (2013). Performance analysis of the storm water management and road tunnel-SMART in Kuala Lumpur. *International Journal of Water Resources and Environmental Engineering*, *5*(7), 410–417. https://doi.org/10.5897/IJWREE2013.0390

Wan Mohtar, W. H. M., Abdullah, J., Abdul Maulud, K. N., & Muhammad, N. S. (2020). Urban flash flood index based on historical rainfall events. *Sustainable Cities and Society*, *56*, 102088. https://doi.org/10.1016/j.scs.2020.102088

Wing, O. E. J., Bates, P. D., Neal, J. C., Sampson, C. C., Smith, A. M., Quinn, N., Shustikova, I., Domeneghetti, A., Gilles, D. W., Goska, R., & Krajewski, W. (2019). A new automated method for improved flood defence representation in large-scale hydraulic models. *Water Resources Research*, *55*(12), 11007–11034. https://doi.org/10.1029/2019WR025957

Wing, O. E. J., Bates, P. D., Sampson, C. C., Smith, A. M., Johnson, K. A., & Erickson, T. A. (2017). Validation of a 30 m resolution flood hazard model of the conterminous United States. *Water Resources Research*, *53*(9), 7968–7986. https://doi.org/10.1088/1748-9326/aaac65

Wing, O. E. J., Bates, P. D., Smith, A. M., Sampson, C. C., Johnson, K. A., Fargione, J., & Morefield, P. (2018). Estimates of present and future flood risk in the conterminous United States. *Environmental Research Letters*, *13*(3), 1–7. https://doi.org/10.1088/1748-9326/aaac65

Wood, D. J., Brown, C. R. M., Doyle, L., Smith, H. L., Waller, S., & Weller, E. F. (2021). Identification of river defences from digital terrain models using deep learning. Science and Practice for an Uncertain Future. https://doi.org/10.3311/FloodRisk2020.14.4

How to cite this article: Massam, A., Smith, H., Filipova, V., Waller, S., Muhamad, N., & Pereira, J. J. (2023). Flood risk in Kuala Lumpur, Malaysia: A consideration of flood defences in a broadscale hydraulic model. *Journal of Flood Risk Management*, *16*(3), e12907. https://doi.org/10.1111/jfr3.12907